Analysis and Verification of 1300 UTC Storm Prediction Center Convective Outlooks

Geoffrey Marion and Jeffrey Frame

Department of Atmospheric Sciences, University of Illinois at Urbana-Champaign, Urbana, IL

1. Introduction

A primary concern of weather researchers, storm spotters, and emergency managers is the risk of severe weather, particularly tornadoes. One product widely used to assess this risk is the Storm Prediction Center (SPC) 1300 UTC Convective Outlook. This outlook may allow for the anticipation of the localized tornado risk and for the subsequent deployment of research equipment or preparation of emergency services. Forecasts that do not verify may lessen the perceived seriousness of future possible severe weather events by the public and emergency managers and result in the misallocation of resources by researchers. Thus, it could be fruitful to identify current challenges in tornado prediction to hopefully improve future forecasts. The primary focus of this research is to analyze these 1300 UTC tornado outlooks to determine meteorological reasons why forecasts for significant tornadic activity did not verify.

2. Methodology

The forecasts investigated herein include all 1300 UTC SPC convective outlooks issued between 3 March 2006 and 3 March 2014 which fit the following categories: Moderate Risk Outlooks, High Risk Outlooks, and any Slight Risk Outlooks with 10% or greater tornado probability. These outlooks were subjectively examined to determine how well the forecasts correlated with the number of tornado reports within the highest risk area. To do this, the highest tornado risk area in each outlook was examined along with the daily tornado reports. An average of the tornado reports for each tornado risk percentage was determined for use in establishing verification. For example, outlooks with a 10% risk of a tornado within 25 miles of a point were examined to develop a general expected number of tornado reports for this risk percentage. The cases reviewed produced a set of 100 outlooks which were determined to be “false alarm” tornado forecasts.

Archived WSR-88D radar data from each of these 100 cases were inspected to identify the dominant storm mode within the highest risk outlook area. For cases in which multiple storm modes existed during the time period covered by the outlook, the storm mode identified in the outlook to potentially produce the most tornadoes was used in the analysis. If this predicted storm mode did not occur, the primary (i.e., most common) storm mode was used. This analysis yielded categories in which these outlooks could fall into based upon the storm mode identified: Linear convection (LC), non-tornadic supercellular convection (NTSC), non-severe convection (NSC), and lack of convective initiation (LCI).

One variable analyzed for LC cases that might explain the lack of tornadoes in certain cases was the angle between the 0-6 km bulk wind shear vector and the initiating boundary. For each case, the 0000 UTC surface frontal analysis was retrieved from the Weather Prediction Center (WPC) archive and the corresponding 0-6 km bulk shear vector analysis was retrieved from the SPC mesoanalysis archive. These maps were overlaid and scaled, and the boundary was traced along with the bulk shear vectors within the highest tornado risk region.

Tangent lines to the boundary were drawn at each location where an analyzed shear vector crossed the boundary. The angle between these lines was used to establish a range of crossing angles. These ranges were put into different categories: 0-30°, 31-60°, 61-90°, and varying angles (the angle range not well situated within one category). Another variable analyzed for these cases was the type of initiating boundary, and the cases were categorized based upon the boundary type: Cold front (CF), warm front (WF), dryline (DL), and stationary front (SF).

For NTSC cases, the mesoanalysis archive was again used to examine lifting condensation level (LCL) heights (Edwards and Thompson 2000) as well as 0-1 km storm relative helicity (SRH; Markowski et al. 1998). A range of values for each of these parameters was determined in the highest tornado risk area, which was averaged for analysis purposes. Categories were established for these averaged values for each variable. The categories for LCLs were less than 1000 m, 1000-1499 m, and greater than 1500 m. The categories for SRH values were less than 100 $m^2 s^{-2}$, 100-199 $m^2 s^{-2}$, and above 200 $m^2 s^{-2}$.

3. Case Study I: 21 May 2013

On 21 May 2013, the SPC issued a Moderate Risk Outlook with a 10% hatched tornado probability indicating a risk of significant tornadoes (EF2 or greater) from southwestern Arkansas to central Texas. The mode of failure for this day was LC (Fig. 1a). A cold front (Fig. 1b) was situated over Texas, providing the trigger for storms. Convective initiation occurred in the morning, and the storms quickly formed a line. This line persisted across the outlook region throughout the day. No tornado reports were received (Fig. 1c). The 0-6 km bulk shear within the highest tornado

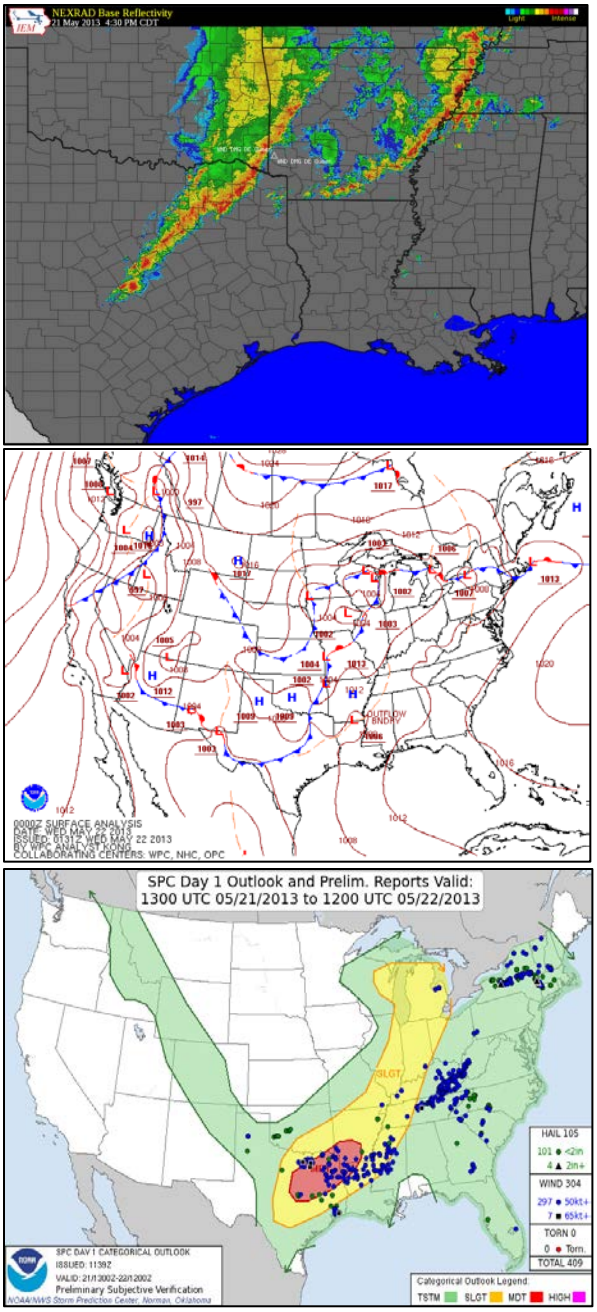

Figure 1. (a) WSR-88D composite reflectivity from 2130 UTC 21 May 2013. (b) WPC surface analysis valid at 0000 UTC 22 May 2013. (c) SPC Convective Outlook from 1300 UTC 21 May 2013 with storm reports superposed. Red dots indicate tornado reports, blue dots indicate high wind reports, and green dots indicate large hail reports.

risk area was between 40 to 60 kts (not shown), and the angle between the bulk

shear vector and the cold front ranged from 30° along the northern portion of the cold front to 55° farther the south. The strong linear forcing for ascent commonly associated with cold fronts was responsible for the rapid upscale growth into a line, despite appreciable 0-1 km SRH (~200 $m^2 s^{-2}$) and low LCLs (~750 m; not shown).

4. Case Study II: 18 February 2009

On 18 February 2009, the SPC issued a Moderate Risk Outlook with 10% hatched (hatching is indicative of a 10% or greater probability of an EF-2 or stronger tornado within 25 miles of a point) tornado probability over parts of the southeastern continental United States (Fig. 2a). The mode of failure for this event was NTSC (Figs. 2b and 2c). Convection initiated south of a stationary front in Mississippi, and these storms developed into supercells within the highest tornado risk region over Alabama (Fig. 2c). The average 0-1 km SRH for this event was 300 $m^2 s^{-2}$, and the average LCL height was 1000 m. All supercells within the highest tornado risk region were non-tornadic, but supercells produced multiple tornadoes just east of this highest risk area in northern Georgia, (Figs. 2a and 2b). The 0-1 km SRH was higher over northern Georgia (~450 $m^2 s^{-2}$) and the LCLs were lower there (~500 m). It is possible that the numerical weather prediction models failed to develop surface-based instability over northern Georgia, resulting in this unverified forecast.

5. Results

The distribution of storm modes for all cases (Fig. 3a), indicates that the plurality (41%) were LC, followed by NSC (35%). NTSC (13%), then LCI (4%), along with a single case of a landfalling tropical cyclone (1%). The graph of the occurrence of these storm modes over time (Fig. 3b) depicts clear temporal trends in these data. NTSC cases exhibit a decrease over time,

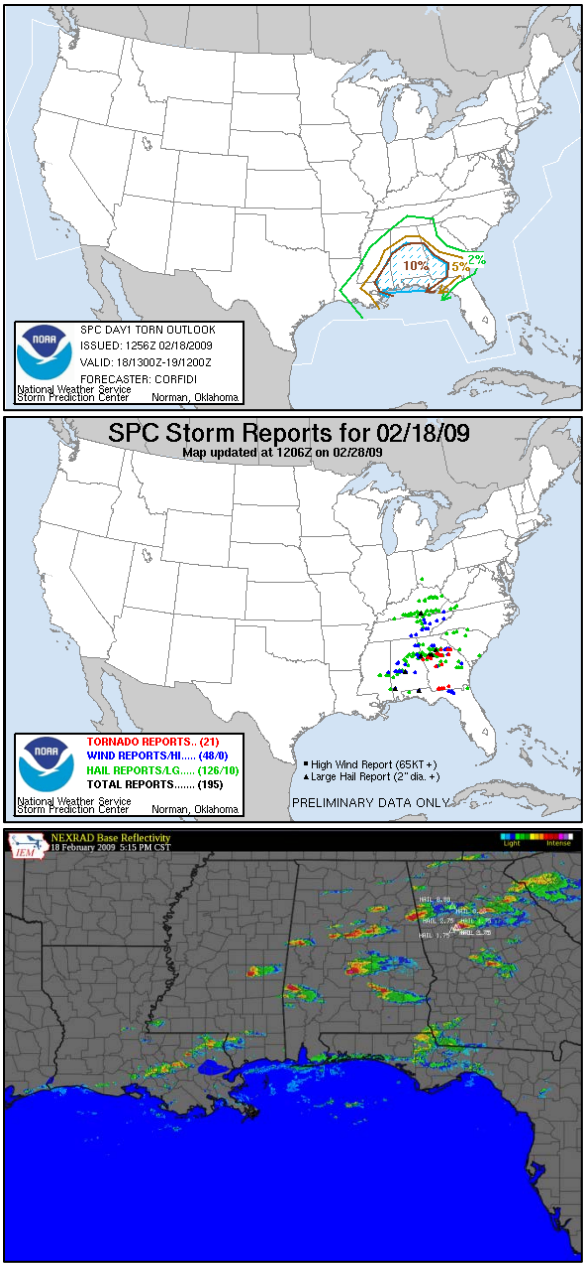

Figure 2. (a) SPC tornado outlook issued 1300 UTC 18 Feb 2009. (b) Preliminary storm reports for the period 1200 UTC 18 Feb 2009 – 1200 UTC 19 Feb 2009. Dots are color coded as in Fig. 1. (c) WSR-88D composite reflectivity from 2315 UTC 18 Feb 2009.

becoming relatively rare (one case in four years) at the end of the study period, possibly indicating improvement in forecasting these events. LC cases also display a slight decrease in frequency over

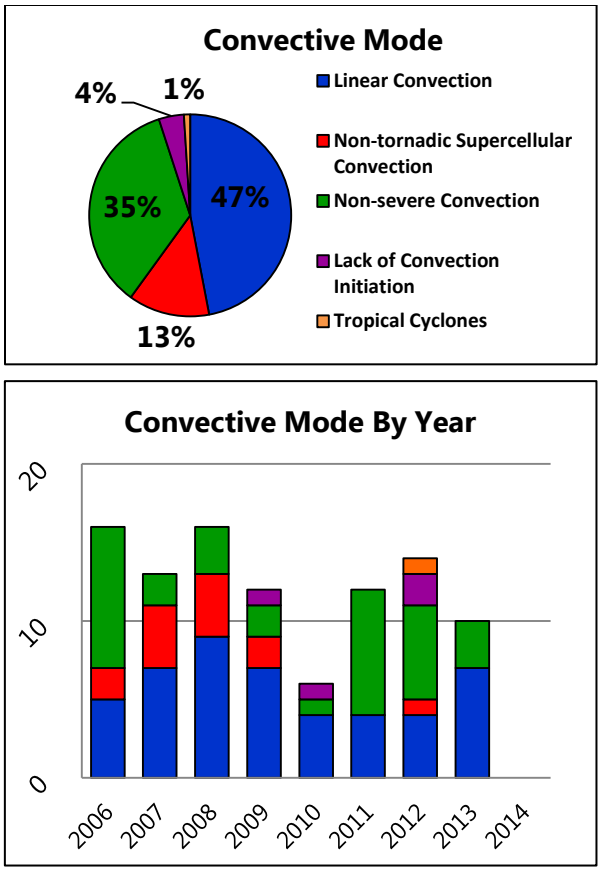

Figure 3. (a) Distribution of the convective mode for all cases. (b) Trend in convective mode over the study period. Color scale in (b) is the same as that in (a).

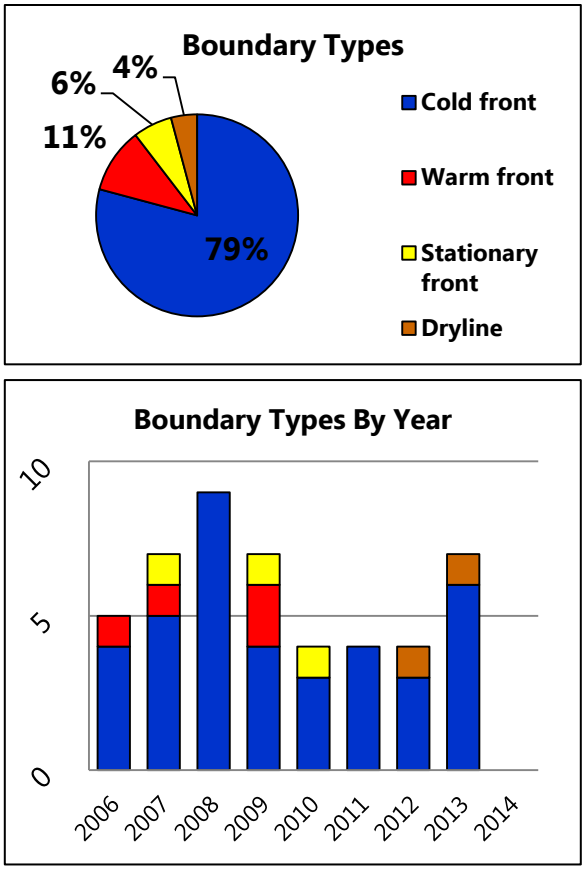

Figure 4. (a) Distribution of the type of initiating boundary for LC cases only. (b) Trend in boundary type for LC cases over the study period. Color scale in (b) is the same as that in (a).

the time period; however, instances of NSC and LCI do not display any apparent trend in frequency.

To further discern possible reasons why there were few tornadoes reported in many of the LC cases, the type of initiating boundary for each case was determined from the WPC analyses. Not surprisingly, CFs (Fig. 4a) constituted a majority (79%) of triggering boundaries for LC cases. The other three boundary types, WFs (11%), SFs (6%), and DLs (4%), are responsible for similar percentages of LC, but far less than CFs. This is not a surprising result owing to the strong linear forcing for ascent often associated with cold fronts and the possibility that the front undercuts the developing storms, causing them to become elevated atop the postfrontal air mass. No trend is evident in the type of initiating boundary over time (Fig. 4b).

Since the magnitude of the 0-6 km bulk shear vector for the vast majority of these cases was sufficient for organized convection (Thompson et al. 2003), the orientation of the shear vectors relative to the initiating boundary were examined. It has been demonstrated that linear convective modes are more likely when the bulk shear vector is approximately parallel to the initiating boundary and that discrete storms are more likely when the shear vector crosses the boundary at a large angle (Dial et al. 2010). Disregarding the cases for which the orientation angles varied significantly

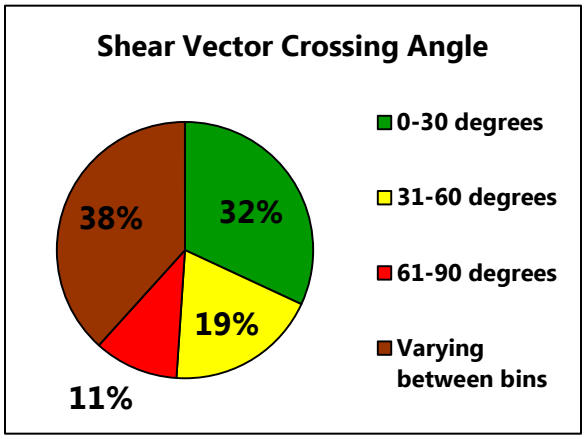

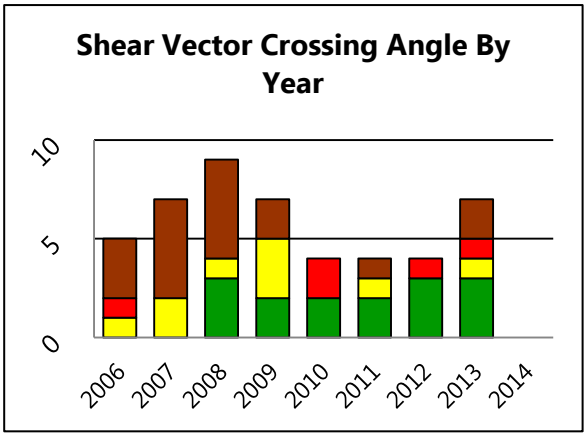

Figure 5. (a) Distribution of the angle at which the 0-6 km bulk shear vector crossed the initiating boundary for LC cases only. (b) Trend in crossing angle for LC cases over the study period. Color scale in (b) is the same as that in (a).

between categories (Fig. 5a), the most common crossing angle range is 0-30° (32%). Crossing angles that ranged between 31-60° and 61-90° occurred less often (19% and 11% respectively). A slight downward trend in the occurrence of 0-30° orientation angles exists over the time period (Fig. 5b), but no trend is evident with the 31-60° and 61-90° crossing angles.

Two variables that have demonstrated skill in discriminating between tornadic and nontornadic supercell environments include 0-1 km SRH (e.g., Markowski et al. 2003) and LCL height (e.g., Edwards and Thompson 2000). These parameters were thus examined for all NTSC cases (Fig. 6). Somewhat

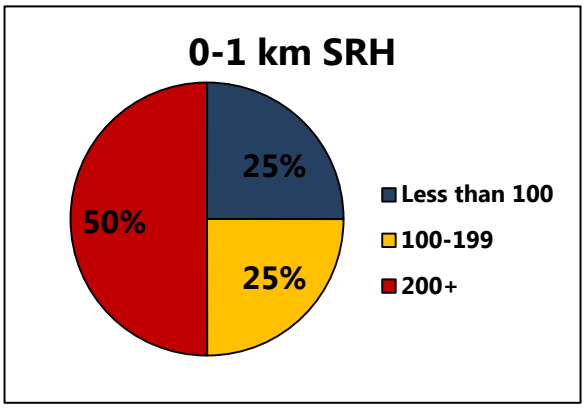

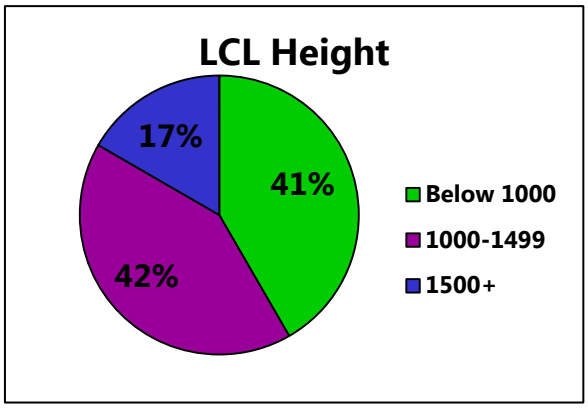

Figure 6. (a) Distribution of the 0-1 km SRH ($m^2 s^{-2}$) for NTSC cases only. (b) Distribution of the LCL height (m) for NTSC cases only.

surprisingly, events with SRH greater than 200 $m^2 s^{-2}$ constitute 50% of all NTSC cases, whereas cases with SRH less than 100 $m^2 s^{-2}$ and events with SRH between 100 and 200 $m^2 s^{-2}$ each account for only 25% of these cases. LCL values below 1000 m comprise 41% of the NTSC cases which is also somewhat unexpected. LCLs between 1000-1499 m account for 42% of these events, and LCLs over 1500 m constitute the last 17% of the events.

6. Conclusions

Instances of only NTSC occurring when tornadoes were forecasted have decreased over time; however, no noticeable temporal trend exists for any other convective modes investigated.

For LC, 0-6 km bulk shear vectors with boundary crossing angles between 0-60° constitute the majority of the cases, which is expected (Dial et al. 2010). The number of forecasts including these angles increased over the period studied. Additionally, cold fronts were responsible for most of the LC cases which is also expected. Predicting tornadoes in association with cold fronts still remains a forecasting challenge.

Surprisingly, half of all NTSC environments were characterized by high 0-1 km SRH (greater than 200 $m^2 s^{-2}$); the LCLs were below 1500 m in most of these cases as well. It is possible that the meoscale environment was not captured well by the numerical weather prediction models in these cases.

To discern specific causes of the lack of tornadoes in these cases, individual events must to be examined to identify other severe weather parameters and pattern-specific storm evolutions which may be case specific. It is our hope that a detailed examination of such events will further improve tornado forecasting in the future.

Acknowledgements

We are grateful to the Department of Atmospheric Sciences at the University of Illinois for providing financial support.

References

Dial, G., J. Racy, R. Thompson, 2010: Short-term convective mode evolution along synoptic boundaries. *Wea. Forecasting*. **25**, 1430-1446.

Edwards R., R. Thompson, 2000: RUC-2 supercell proximity soundings, part II: An independent assessment of supercell forecast parameters. Preprints, *20th Conf. on Severe Local Storms*, Orlando, FL, Amer. Meteor. Soc., 435-438.

Markowski, P., C. Hannon, J. Frame, E. Lancaster, A. Pietrycha, R. Edwards, and R. Thompson, 2003: Characteristics of vertical wind profiles near supercells obtained from the Rapid Update Cycle. *Wea. Forecasting*. 18, 1262-1272.

____, E. Rasmussen, J. Straka, 1998: The occurrence of tornadoes in supercells interacting with boundaries during VORTEX-95. *Wea. Forecasting*. 13, 852-859.

Thompson, R., R. Edwards, J. Hart, K. Elmore, and P. Markowski, 2003: Close proximity soundings within supercell environments obtained from the Rapid Update Cycle. *Wea. Forecasting*. 18, 1243-1261